Ligand-Induced Structural Evolution of Pt_{55} Nanoparticles: Amine *versus* Thiol

Ji Hoon Ryu,[†] Sang Soo Han,[‡] Da Hye Kim,[†] Graeme Henkelman,[§] and Hyuck Mo Lee[†,*]

[†]Department of Materials Science and Engineering, KAIST, 291 Daehak-ro, Yuseong-gu, Daejeon, 305-701, Republic of Korea, [‡]Center for Nanocharacterization, KRISS, 267 Gajeong-ro, Yuseong-gu, Daejeon, 305-701, Republic of Korea, and [§]Department of Chemistry and Biochemistry, The University of Texas at Austin, Austin, Texas 78712-0165, United States

ABSTRACT We report the geometric and electronic effects of amine (with one lone pair electron) and thiol (with two lone pair electrons) ligands on the structural transformation of Pt_{55} nanoparticles (NPs) by first-principles calculation. Although a cuboctahedral (COh) structure is less stable than an icosahedral (Ih) structure by 1.36 eV for a bare Pt_{55} NP, the activation barrier from the COh to the Ih structure is very high, by 1.97 eV, indicating that it would be difficult to observe the structural evolution of a COh structure to an Ih structure for a bare Pt_{55} NP at ambient temperature. However, with the help of the adsorption of methylamine, the structural evolution from a COh structure to an Ih structure is accomplished by the Mackay transformation. This transformation is driven by a combination of both the external forces resulting from the adsorption of the ligand, which pull out the Pt atoms on the face sites of NPs in a radial direction, and the contraction forces in a tangential direction. As more methylamine is added, the Ih structure is observed to return to the original COh structure owing to the directional orbital hybridization that occurs between the Pt NPs and the methylamine. In contrast, such structural evolutions are not observed in the case of methylthiol because the sulfur (S) in the ligand has two lone pair electrons, leading to two Pt—S bonds. As a result, the radial-directed external force that the NPs experience because of the adsorption of methylthiols is much lower than that found in methylamine-ligated NPs. Furthermore, the adsorption of methylthiol leads to an expansion (not contraction) in the tangential direction, which does not qualify as a Mackay transformation. Thus, the Pt NPs ligated with methylthiol do not have a driving force strong enough to cause structural change. The methylthiol-stabilized Pt NPs retain their initial COh structure despite an abundance of ligand adsorption. From these results, we suggest that the NP structure can be controlled by varying the amount and species of ligands.

KEYWORDS: density functional theory · Pt nanoparticle · ligand adsorption · structural evolution · amine · thiol

Metal nanoparticles (NPs) have been the subject of extensive investigation in recent years because of their technological importance in many areas of physics and chemistry. Generally, the chemical reactivity[1−3] of NPs strongly depends on the interplay between their geometric structure and electronic structure, which is dependent on the size and shape of the NPs. Because of this dependency, NPs are known to have unique properties that are different from the bulk. It is therefore essential to investigate the synthetic process that yields nonagglomerated, uniform NPs with a well-controlled mean size and a narrow size distribution. A key factor in the production of uniform NPs is the ability to keep them physically isolated by avoiding irreversible aggregation. Stable isolated metallic NPs can generally be obtained through the use of various capping agents. Denoted as ligands in this study, these agents, which includes amines and thiols, bind to the NP surface, where they prevent aggregation and make the NPs soluble in various solvents.[4−18]

In general, ligands were believed to attach to the surface of NPs through a weak interaction.[18,19] Based on such belief, the traditional view of ligands is held that they have no significant effect on the geometric and the electronic structure of NPs. In recent years, however, many studies have revealed that ligands can affect the geometric and electronic structure of metallic NPs[8,11−16,20,21] as well as the catalytic properties.[22] In particular, several studies have reported that the stability of metal NPs can be dramatically changed by the adsorption of ligands. Pei *et al.*[22] showed that $(PPh_3)_{12}Cl_6$ ligands (PPh_3 = triphenylphosphine) can effectively stabilize the quasi-Ih-Au_{55} core structure. This structure can significantly affect the electronic structure of the inner gold NP, which leads to catalytic activity. Rahman and co-workers[16] also reported that clean Au NPs with a planar structure have the lowest total energy, whereas the Ih structure exhibits the lowest total energy when the NPs are ligated with phosphine. The structural stability of ligated Au NPs primarily depends on the number of ligands adsorbed as a result of the ligand-induced charge transfer from the surface Au—Au to the Au—ligand bonds, which makes strong Au—ligand covalent bonds. Similar to the present study, Rodriguez *et al.*[15] found that a bare Pt_{55} NP will experimentally undergo a severe structural evolution as more ligands are added. Isolated and

* Address correspondence to hmlee@kaist.ac.kr.

Received for review January 2, 2011 and accepted October 1, 2011.

Published online October 01, 2011
10.1021/nn202757r

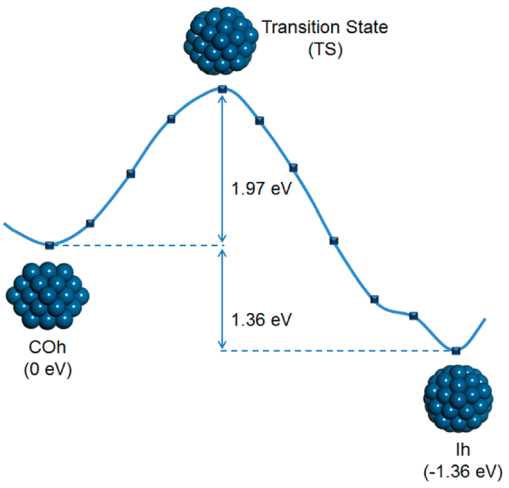

Figure 1. Optimized structures and transition state (TS) during the structural transformation from a COh structure to an Ih structure. Denoted energies are relative to the energy of a COh structure.

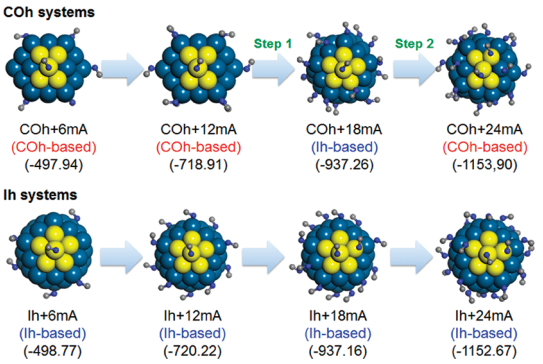

Figure 2. Structural evolution of Pt_{55} NPs in COh and Ih systems with the number of methylamines. The FCC and Ih motifs are represented by the yellow atoms in the COh+6 mA system and the Ih+6 mA system, respectively. The values in parentheses refer to the total energy of the system (E_{total}, eV).

stable 1.2 nm Pt NPs with an FCC structure initially change to an Ih structure and then revert to the FCC structure following the addition of 0.2 equiv of PPh_3 ligand. Despite its scientific importance, however, the detailed mechanism and driving force of this structural transformation between FCC and Ih structures are not fully understood.

In general, the adsorption properties of ligands depend on the electronic nature of ligands as well as the amount and species of ligands present. Thus, a detailed investigation of the interaction between ligands and NPs should shed light on the nature of ligand-stabilized NPs and provide important knowledge on how to control the geometric and electronic structure of NPs. We thus aim to use computational methodologies to examine how the structure of Pt_{55} NPs evolves with the number and variety of ligands.

In this work, we study the structural evolution of Pt_{55} NPs that are induced by two different ligands: methylamine (NH_2CH_3) and methylthiol ($SHCH_3$). Because the two ligands have different electronic natures (*e.g.,* one lone pair electron for methylamine *versus* two lone pair electrons for methylthiol), their binding properties on the NP surface must be different, even though both methylthiol and methylamine adsorb to the NP surface in equal amounts. Thus, adsorption of each ligand leads to a different effect on the structures of the amine- or thiol-stabilized Pt NPs. In this study, we find that the methylamine-stabilized Pt NPs experience two structural changes, which are dependent on the amount of adsorbed methylamines. In contrast, methylthiol tends to simply expand NPs without causing any structural changes.

RESULTS AND DISCUSSION

Structural Evolution of Pt NPs with Varying Numbers of Methylamines. We have investigated the structural transformation between a COh structure and an Ih structure of a bare Pt_{55} NP. Figure 1 shows both the optimized structures and transition state (TS) during the structural transformation from a COh structure to an Ih structure. In this figure, the energy of the COh structure is 1.36 eV higher than that of the Ih structure, and the energy barrier for the structural transformation (COh to Ih) is 1.97 eV. This result indicates that the structural change from a COh structure to an Ih structure is kinetically unfavorable, although equilibrium thermodynamics favor the transformation.

In addition to a bare Pt_{55} NP, we investigated the binding natures of a methylamine on a Pt_{55} NP. In general, a methylamine molecule prefers to form a single bond with a surface Pt atom because methylamine has one lone pair electron. A methylamine adsorbs at one of three different top sites on the surface of the Pt NPs: the vertex, the edge, or the face (Figure S1 in the Supporting Information). The adsorption energies of a methylamine are 1.66 eV at the vertex, 1.33 eV at the edge, and 1.22 eV at the face, which are inversely proportional to the coordination number of each of the adsorption sites (Figure S1). As usual, the adsorbed ligand will pull out the ligated metal atoms from the surface when the ligand interacts with the surface metal atom.[12−14,21] Methylamine also displays similar behavior, as summarized in Figure S1. Here, note that the pulling distance on the face site is larger than that of other sites, although it has the lowest adsorption energy.

Charge transfer could be another property of the methylamine-ligated Pt_{55} NP. Bader charge analysis shows that 0.28 electron in a methylamine goes to a Pt NP when a single methylamine is attached to the vertex site. As a result, the Fermi level (E_F) of the Pt NPs increases as the number of adsorbed methylamines increases. The source of this charge transfer could be explained by the coordinate covalent bond between the methylamine

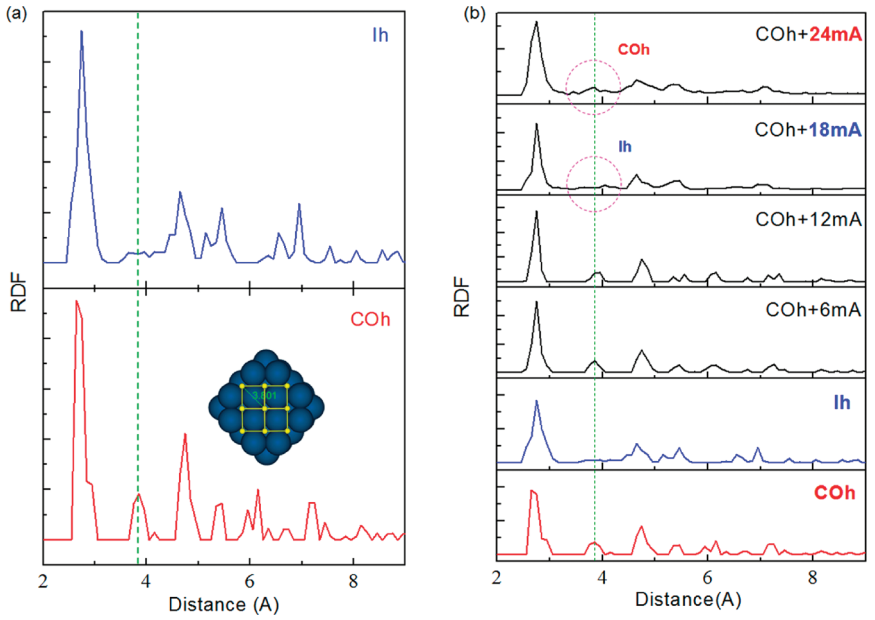

Figure 3. RDF analyses for (a) bare COh and Ih structures of Pt_{55} and (b) COh structures ligated by methylamines.

and the Pt NPs. This bond is formed by the lone pair electrons in the methylamine.

Because of these facts, we examined the structural change of Pt_{55} NPs with both a COh structure and an Ih structure varying the number of methylamines (6, 12, 18, and 24), which is shown in Figure 2. Here, the methylamine is denoted as "mA". The COh NPs retain their initial structure in COh+6 mA and COh+12 mA systems, where all of the methylamines position the vertex site. However, when six additional methylamines are added to the COh+12 mA system (COh+18 mA), the COh structure undergoes a severe structural transformation and then becomes an Ih-based structure (step 1). Here, the added methylamines position themselves on the face sites rather than the edge sites owing to the repulsive force exerted by the existing 12 methylamines (Table S1), although methylamines prefer to attach to an edge site rather than to a face site (Figure S1). In addition, if six additional methylamines are added to the COh+18 mA system (COh+24 mA), the Pt_{55} NP experiences another structural transformation from an Ih-based structure to a COh-based structure (step 2), in which all of the added methylamines seek the edge sites. For all Ih systems, however, the Pt NP retains its original Ih structure no matter how much the number of ligands increases.

To clarify the structural evolution, we investigated the number of surface FCC and Ih motifs (Table S1). The FCC motif is a symmetrical mirrored structure that usually appears in a COh structure, whereas the Ih motif has a representative 5-fold symmetrical structure. For the COh+6 mA and COh+12 mA systems, there is no structural evolution; in other words, they keep the original COh structure with 12 FCC motifs on the surface. For the COh+18 mA system, however, there are eight Ih motifs on the surface, indicating that Pt NP in the COh+18 mA system is based on an Ih structure. In the case of COh+24 mA, the NP has 10 FCC motifs on its surface, indicating that the Pt NP in the COh+24 mA system returns to the original COh structure from an Ih-based structure. The number of FCC and Ih motifs on the COh surface supports the notion that the structure of COh NPs evolves with the number of methylamines.

An analysis of the radial distribution function (RDF) also enables us to collect more detailed and accurate information on the structures of Pt NPs in the COh+18 mA and COh+24 mA systems. Figure 3 shows the RDF peaks of a bare COh (the red line), a bare Ih (the blue line), and other ligated COh systems. In Figure 3a, we can clearly distinguish the COh peaks from the Ih peaks by the unique peak that appears around 3.8 Å. This peak is caused by the (100) surface on the COh structure. As shown in the inset of Figure 3a, in the COh+18 mA peaks, the peak disappears because the Pt NP has evolved to an Ih structure; however, it reappears in the COh+24 mA system because the Pt NP in this system has reverted to a COh structure. This RDF result is in good agreement with results of previous motif analysis.

Step 1: Structural Evolution from the COh-Based Structure to the Ih-Based Structure by 18 Methylamines. In Figure 2, we showed that six additional methylamines lead to the structural transformation from the COh structure with 12 methylamines to the Ih-based structure with 18 methylamines. In general, the Mackay transformation[23] is a well-known structural transformation mechanism between the COh and Ih structures, where a COh structure can be distorted to an Ih structure when the distance between the vertices and the center uniformly contracts by 5% and then each of the (100) square faces splits into two (111) equilateral triangles.

Figure 4 represents the atomic pathway on the (100) surface of a Pt_{55} COh NP during the Mackay transformation. Here, the red arrow indicates the pathway (radial movement) of the face atoms, and the green and blue arrows indicate the pathways (tangential movement) of the vertex and edge atoms, where the movement of Pt atoms is vertical and along the NP surface, respectively.

We summarize the distance (D_c) from the center of ligated Pt_{55} NPs to each adsorption sites (vertex, edge, and face) in Table 1. The D_c values for the vertex and edge atoms in the bare NP system are relatively small: the changes are −3.7% and −1.5%, respectively, where a negative change indicates a contraction of the NP after transformation. The contraction of 3.7% at a vertex site is near the condition (5%) for the Mackay transformation. On the other hand, the D_c value for the face site in the bare NP system increased by as much as 13.6%. During the transformation from a COh structure to an Ih structure, the most prominent change is a pulling of the Pt atoms out of face sites, although the contraction of vertex sites is also an important factor, as noted by A. L. Mackay.[23] These results suggest that external forces that pull the Pt atoms out of face sites in a radial direction are the driving force for the structural evolution from a COh to an Ih.

Table 1 also shows the D_c values in the COh+12 mA and COh+18 mA systems. The changes in D_c for the vertex and edge atoms are small, at −1.3% and −1.7%, respectively. However, the corresponding change for the face atom is very large, +12.3%. These results are similar to the results of the bare NP system based on the Mackay transformation. Therefore, we can deduce that the structural transformation exhibited by Pt_{55} NPs of the COh+18 mA system from a COh to an Ih configuration is due to the geometric effect caused by methylamine ligands.

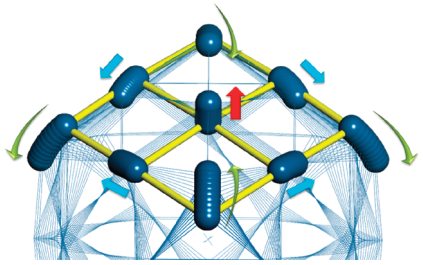

Figure 4. Atomic pathway during a structural transformation from a COh structure to an Ih structure. The yellow line denotes the (100) face of the initial COh structure.

Step 2: Structural Evolution from the Ih-Based Structure to the COh-Based Structure by 24 Methylamines. In Figure 2, step 2 refers to another structural transformation observed in the COh+24 mA system. In this case, when six additional methylamines are added to the edge sites of the NP in the COh+18 mA system, the NP undergoes a structural evolution from an Ih-based structure to a COh-based structure. This structural transformation is the reverse process of step 1. To determine the origin of this transformation, we revisited the Mackay mechanism and analyzed the atomic movement in the radial and tangential directions during the structural evolution. As already mentioned, step 1 is based on the Mackay transformation, which occurs when the ligated Pt atoms are pulled out of the face sites in a radial direction. In step 2, however, no noticeable change occurs on any of the vertex, edge, and face sites because of the adsorption of additional methylamines. During step 2, the radial movement at the face site is only 1.53%, which is much smaller than the radial movement found during step 1 (12.3%). Moreover, all tangential movement at the vertex and edge sites is positive, indicating that the Pt_{55} NP is expanding. Accordingly, step 2 does not satisfy the condition of the Mackay transformation, indicating that the structural evolution of step 2 is not the reverse of the Mackay transformation.

We therefore focused on the electronic structure of the ligated Pt_{55} NP instead of the geometric effects in order to understand step 2. Several studies have reported that the structural stability of transition metal NPs strongly depends on the s−d hybridization owing to relativistic effects.[24−26] Therefore, we not only calculated the Pt_s-Pt_d hybridization of Pt_{55} NPs but also considered Pt_d-N_p hybridization because the binding nature between a methylamine and a Pt atom is usually dominated by the interaction of the *d-orbital* in a Pt atom (Pt_d) and the *p-orbital* in an N atom (N_p) of a methylamine ligand. To make these orbital hybridizations more quantitative, we defined the Pt_s-Pt_d hybridization as $I_{sd}\Sigma_N^{SS} = \int_{-\infty}^{E_F} \rho_N^s(\varepsilon)\, \rho_N^d(\varepsilon)\, d\varepsilon$ (ρ^s, ρ^d: s and d density of states of the Nth Pt atom) and the Pt_d-N_p hybridization as $I_{dp} = \Sigma_N^L = \int_{-\infty}^{E_F} \rho_{Pt}^d(\varepsilon)\, \rho_N^p(\varepsilon)\, d\varepsilon$ (L, $\rho_{Pt}{}^d$, $\rho_N{}^p$: the number of ligands, d and p density of states of the Pt atom and N atom, respectively).

The COh+24 mA system has many methylamines that interact on the NP surface with a high coverage of more than 0.5. We therefore postulated that the

TABLE 1. Distance (D_c) from the Center of NPs to Each Adsorption Site and D_c Changes in Three Systems: The Bare NP, COh+18 mA, and COh+24 mA Systems

	bare NP			COh+18 mA (step1)			COh+24 mA (step2)		
site	COh (Å)	Ih (Å)	changes (%)	COh+12 mA (Å)	COh+18 mA (Å)	changes (%)	COh+18 mA (Å)	COh+24 mA (Å)	changes (%)
vertex	5.35	5.15	−3.7%	5.37	5.30	−1.3%	5.30	5.33	+0.57%
edge	4.74	4.67	−1.5%	4.78	4.70	−1.7%	4.70	4.77	+1.49%
face	4.11	4.67	+13.6%	4.07	4.57	+12.3%	4.57	4.64	+1.53%

TABLE 2. Total Energy, I_{sd}, I_{dp}, and Adsorption Energy (E_{ad}) for the COh+24 mA System and the Ih+24 mA System

	energy (eV)	I_{sd}	I_{dp}	E_{ad} (eV)
COh+24 mA	−1153.90	12.13	4.90	−0.48
Ih+24 mA	−1152.67	12.08	4.56	−0.29

electronic interaction between methylamines and NPs in this system would be more important than any other system and subsequently conducted a more detailed analysis of the binding properties of methylamines in the COh+24 mA system. As mentioned in the previous paragraph, the p-orbital in an N atom of methylamine interacted strongly with the d-orbital in a Pt atom on the NP surface. The strong directionality in each orbital requires that the surface Pt atoms and methylamines be rearranged to match the directionality between the two orbitals and allow stronger binding. However, methylamines are difficult to rearrange on their own, owing to the strong repulsive force caused by the abundance of already adsorbed methylamines in the COh+24 mA system. Instead, the surface Pt atoms and methylamines are rearranged together to match the directionality between the two orbitals, Pt_d and N_p. This allows the methylamines to strongly interact with the Pt atoms, yielding a high d−p hybridization (I_{dp}) and, thus, a high level of adsorption energy.

Table 2 shows the total energy, I_{sd}, I_{dp}, and the adsorption energy (E_{ad}) of a methylamine in the COh+24 mA and Ih+24 mA systems. The total energy of the COh+24 mA system is lower (indicating greater stability) than that of the Ih+24 mA system, which is correlated with I_{sd} and I_{dp}. In particular, the I_{dp} index in the COh+24 mA system is 4.90, which is 7.5% larger than the I_{dp} value of 4.56 in the Ih+24 mA system. Because the I_{dp} index refers to the interaction of ligands and Pt NPs, the higher I_{dp} index in the COh+24 mA system indicates a stronger binding between the Pt and ligands. Indeed, the adsorption energy of a methylamine in the COh+24 mA system is 0.48 eV, which is higher than that in the Ih+24 mA system. From these results, we find that the surface Pt atoms on an Ih-based structure are rearranged to a COh-based structure because of the stronger directional bonds between the d-orbital in Pt and the p-orbital in N. Accordingly, the structural transformation observed in the COh+24 mA system is induced by the electronic effect of methylamines rather than the geometric effect.

These results are supported by a reported experimental observation, where an isolated, stable 1.2 nm Pt NP with an fcc structure becomes an Ih structure and is then changed back to an fcc structure with increasing amount of PPh_3 ligands.[15] Because the phosphine (PPh_3) molecule also has one lone pair electron, similar to the amine referenced in this work, the PPh_3 is

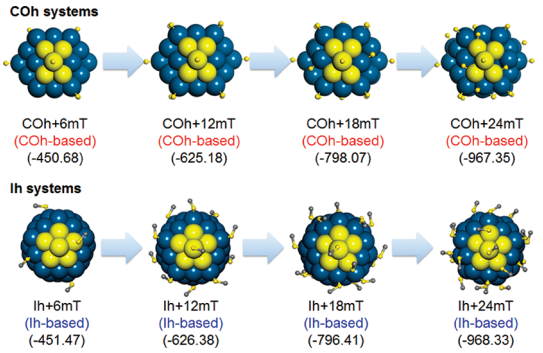

Figure 5. Structures of Pt_{55} NPs in COh and Ih systems with the number of methylthiols. The values in parentheses refer to the total energy of the system (E_{total}, eV).

expected to have a similar electronic nature to the methylamine, which leads to the similar bonding motif. Recent studies support this postulation.[14,22,27] In particular, Periyasamy and Remacle[27] successfully modeled the structure of an experimentally synthesized $Au_{55}(PPh_3)_{12}Cl_6$ as an $Au_{55}(PH_3)_{12}Cl_6$, with PH_3 groups instead of PPh_3 groups owing to the computational cost. Guliamov *et al.* reported[14] that Au_{13} NPs have strained and distorted cluster shapes as a result of on-top phosphine ligands and a combination of on-top and bridging thiol ligands, a claim that is strongly supported by experiments (EXAFS/TEM). These results are in excellent agreement with our postulation that the amine and the phosphine ligands affect the geometry of metal NPs in the same manner. Therefore, although there is not enough direct experimental evidence about structural changes of Pt NPs caused by methylamines, PPh_3 can give a full description of the effect of methylamine on Pt NP's geometry, as seen in the work of Rodriguez *et al.*[15] Hence, we can say that the two structural transformations observed in the experimental study can be explained by the transformation mechanism that we suggested for the methylamine systems given in the present work.

Structural Evolution with the Number of Methylthiols. In contrast to methylamine, methylthiol tends to form two single bonds with two surface Pt atoms because it has two lone pair electrons. The adsorption energies of methylthiol on Pt_{55} NPs are 1.13 eV for the vertex site, 1.10 eV for the edge site, and 1.07 eV for the face site. Owing to low coordination of the vertex atom, the methylthiol makes a single bond at the vertex site with a similar level of stability as other bridge sites. The ligand also pulls out the ligated Pt atom whenever it interacts with a surface Pt atom. The pulling distance after a ligand adsorption is 1.12% on the vertex, 1.90% on the edge sites, and 2.43% on the face sites.

Similar to the methylamine work, we investigated structures of COh with the number of methylthiol. However, there is no noticeable structural transformation, and the Pt NPs retain their initial COh structure (Figure 5). This result was also confirmed by the RDF

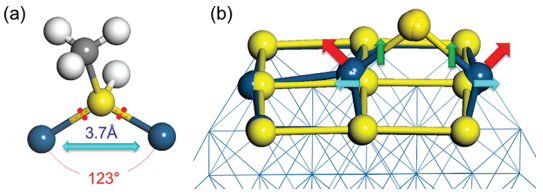

Figure 6. (a) Binding nature of methylthiol with two Pt atoms; (b) pathway of methylthiol-ligated Pt atoms on a (100) face during interaction with methylthiol.

analysis (Figure S2), indicating that one peak (3.8 Å) reflecting the unique property of the COh structure was observed in all the methylthiol-ligated COh systems. We also calculated the D_c values for all surface Pt atoms in the COh, COh+18mT, and COh+24mT systems (Figure S3). The D_c values increase as the methylthiols interact with the Pt NPs, which means that the NPs just expand as the number of methylthiols increases. However, in contrast to previous methylamine systems, this expansion occurs without any structural evolution.

To understand why NPs undergo different behaviors in methylamine and methylthiol systems, we investigated the binding nature of a methylthiol with two Pt atoms. Owing to its two lone pair electrons, the methylthiol binds with two Pt atoms at an angle of about 123° and gives a Pt−Pt distance of about 3.73 Å (Figure 6a). Figure 6b shows the pathway of the methylthiol-ligated Pt atoms on the bridge of (100) face sites during the interaction. The two methylthiol-ligated Pt atoms are subject to a tangential force induced by the binding angle and distance, and this tangential force (indicated by the blue arrows in Figure 6b) propels the Pt atoms along the NP surface. At the same time, the ligated Pt atoms are subject to a radial force induced by the pulling of a methylthiol (indicated by the green arrow in Figure 6b). Both the radial and tangential forces make the ligated Pt atoms pull out in a diagonal direction (indicated by the red arrows in Figure 6b).

The D_c value of the Pt atoms on the face sites in the COh+24mT system is 6.57% greater than that of the bare COh (Table S2), which is much lower than the 13.6% found in methylamine-ligated Pt_{55} NP. Moreover, all of the tangential movement at the vertex and edge site is positive, which does not satisfy the condition for the Mackay transformation. Hence, the combined forces would not possess sufficient driving force to change the NP structure from a COh to an Ih. This evidence supports the conclusion that the binding nature of a methylthiol ligand by two lone pair electrons prevents Pt_{55} NPs with a COh structure from undergoing a severe structural transformation and only expands Pt_{55} NPs when there is an abundance of methylthiol adsorption.

In addition, we can find the relative stability between Ih and COh structures with the interaction of the ligands. As shown in Figure 5, until the addition of 12 methylthiols, Ih is more stable than COh, but the COh+18mT system has lower energy by 1.66 eV than the Ih+18mT system. The Ih structure regains its stability in the 24 methylthiol system. That is, despite the increasing number of ligands, all Pt NPs retain their initial COh and Ih structures, but the relative stability between two structures can be changed. From these results, we can deduce that all of the methylthiol-ligated systems in this study are local minima without any structural change during the interaction.

CONCLUSION

In summary, we have shown that the structure of Pt_{55} NPs changes with the number and species of the adsorbed ligands. When methylamines interact with Pt_{55} NPs with a COh structure, the Pt NPs undergo two severe transformations as the number of methylamines increases. In the first severe transformation (step 1), a COh structure changes into an Ih-based structure. In this step, the geometric effect of the methylamines induces a structural transformation of the Pt NPs by a Mackay transformation mechanism. In the second severe transformation (step 2), the Ih-based structure returns to the COh-based structure, because the surface Pt atoms are rearranged to match the directionality between the d-orbital in the Pt atom and the p-orbital in the N atom to allow strong bonding. The results confirm that the structural transformations of the Pt_{55} NPs are affected by both the geometric and electronic effects of methylamines. However, the two lone pair electrons in methylthiol lead to a bonding nature different from methylamine's. Because methylthiol tends to form two single bonds with two surface Pt atoms, methylthiol-ligated systems would not be able to obtain a driving force sufficient for structural transformation. As a result, the methylthiol-stabilized Pt NPs retain their initial COh structure and experience an expansion only with the addition of methylthiols. Together, these results suggest the possibility that the structure of NPs could be controlled by adjusting the amount and variety of ligands for a practical catalytic application.

COMPUTATIONAL DETAILS

We performed density functional theory calculations within a plane wave basis set,[28] and the projector augmented wave pseudopotential method[29] considering scalar relativistic effects implemented in VASP[30] was used. A kinetic energy cutoff of 450 eV was used for the plane wave basis set and was sufficient

for convergence. In this study, the PW91 functional of a generalized gradient approximation[31] level was used for the exchange−correlation energy. The simulation box for all systems in this study has dimensions of 28 Å × 28 Å × 28 Å. The geometries were optimized with a conjugated gradient method until the forces acting on each ion core were less than 0.01 eV/Å with respect to the size of the vacuum and the k-point mesh. For relaxation of the electronic degrees of freedom, we achieved a total energy convergence of up to 10^{-6} eV. A Gaussian smearing of 0.05 eV was used for all calculations.

For bare Pt NP geometries, we considered two stabilized tructures: a cuboctahedral (COh) and an icosahedral (Ih) structure. In addition, we selected NPs with 55 Pt atoms (Pt_{55}), which were experimentally synthesized.[11,15] For bare NP_{55} structures, two structures with lower energy (and thus greater stability) than the COh and Ih structures were reported: the Rosette structure by Apra *et al.*[32] is lower in energy by 0.483 eV than the Ih structure, and the core and surface reconstructed NP by Silia *et al.*[33] was lower by 5.22 eV than the Ih structure. However, our aim in this study is only to investigate the structural transformation of NPs varying in the type and amount of surface ligands. So we considered the COh and Ih structures that were commonly synthesized in several experiments,[15,18,19] although they are thermodynamically less stable than those suggested by Apra *et al.*[32] and Silvia *et al.*[33] During the synthesis of metal NPs, ligands with a long alkyl chain (*e.g.,* dodecanethiol) are typically used. However, in this work, we considered the shortest carbon chain, methyl ($-CH_3$), as an equivalent to an alkyl chain because of computational limitations.[34,35] In the case of thiol, we refer to the experimental literature.[6,19] In general, thiols can interact with metal NPs in two different ways. The first interaction is the adsorption of the RSH molecule on the surface.[36] The second interaction is the formation of thiolate or disulfides on metal surfaces, which generates RS groups.[37,38] Typically, the RS−H bond is easy to break on Pt NPs,[19] similar to Au NP cases,[12,13,39,40] so it actually exists in the form of RS−, *i.e.*, thiolate, not thiol. However, because the aim of this study is to investigate the structural transformation by the interaction between orbitals of Pt NP and lone pair electrons in surface ligands (one lone pair electron for an amine ligand versus two lone pair electrons for a thiol ligand), we considered the RS−H bond in the thiol ligand to study the effect of only two lone pair electrons in the absence of an unpaired electron (note that a thiolate molecule has not only two lone pair electrons but also a unpaired electron, leading to different chemical binding characteristics from those of thiol).

To obtain the ligated geometry of the ligated Pt_{55} NPs, we attached six ligands of methylamine and methylthiol to the relaxed bare Pt_{55} NPs at several adsorption sites and then selected the ligated NP systems with the lowest energy. In the same way, we added six more ligands to the previously selected systems. Finally, we obtained the lowest energy level for Pt_{55} NPs with 6, 12, 18, and 24 ligands on the surface.

Acknowledgment. This research was supported by Future-based Technology Development Program (Nano Fields) through the National Research Foundation of Korea (NRF) funded by the Ministry of Education, Science and Technology (2010-0019163). The work in Austin is supported by the Department of Energy under contract DE-SC0001876 using computational resources provided by the National Energy Research Scientific Computing Center and the Texas Advanced Computing Center.

Supporting Information Available: Adsorption and structural roperties for the number of ligands, Table S1 for adsorption sites, final structures, and the number of fcc and Ih motifs in COh system with the number of methylamines, Table S2 for distance from the center of NPs to each adsorption site (D_c) and D_c changes for the bare COh system and the COh+24mT system, Figure S1 for three adsorption sites on a Pt_{55} COh NP of a methylamine ligand, Figure S2 for RDF peaks of a bare COh, a bare Ih, and other COh systems, Figure S3 for values of D_c for all surface Pt atoms in the bare COh system, the COh+18mT system, and the COh+24mT system. This material is available free of charge *via* the Internet at http://pubs.acs.org.

REFERENCES AND NOTES

1. Haruta, M. Size- and Support-Dependency in the Catalysis of Gold. *Catal. Today* **1997**, *36*, 153–166.
2. Meyer, R.; Lemire, C.; Shaikhutdinov, S. K.; Freund, H. Surface Chemistry of Catalysis by Gold. *Gold Bull.* **2004**, *37*, 72–124.
3. Valden, M.; Lai, X.; Goodman, D. W. Onset of Catalytic Activity of Gold Clusters on Titania with the Appearance of Nonmetallic Properties. *Science* **1998**, *281*, 1647–1650.
4. Eklund, S. E.; Cliffel, D. E. Synthesis and Catalytic Properties of Soluble Platinum Nanoparticles Protected by a Thiol Monolayer. *Langmuir* **2004**, *20*, 6012–6018.
5. Liu, J. C.; Sutton, J.; Roberts, C. B. Synthesis and Extraction of Monodisperse Sodium Carboxymethylcellulose-Stabilized Platinum Nanoparticles for the Self-Assembly of Ordered Arrays. *J. Phys. Chem. C* **2007**, *111*, 11566–11576.
6. Neouze, M. A.; Schubert, U. Surface Modification and Functionalization of Metal and Metal Oxide Nanoparticles by Organic Ligands. *Monatsh. Chem.* **2008**, *139*, 183–195.
7. Yang, J.; Lee, J. Y.; Deivaraj, T. C.; Too, H. P. An Improved Procedure for Preparing Smaller and Nearly Monodispersed Thiol-Stabilized Platinum Nanoparticles. *Langmuir* **2003**, *19*, 10361–10365.
8. Yang, J.; Lee, J. Y.; Too, H. P. Size Effect in Thiol and Amine Binding to Small Pt Nanoparticles. *Anal. Chim. Acta* **2006**, *571*, 206–210.
9. Yee, C.; Scotti, M.; Ulman, A.; White, H.; Rafailovich, M.; Sokolov, J. One-Phase Synthesis of Thiol-Functionalized Platinum Nanoparticles. *Langmuir* **1999**, *15*, 4314–4316.
10. Ramirez-Meneses, E.; Dominguez-Crespo, M. A.; Montiel-Palma, V.; Chavez-Herrera, V. H.; Gomez, E.; Hernandez-Tapia, G. Electrochemical Characterization of Platinum Nanoparticles Stabilized by Amines. *J. Alloys Compd.* **2009**, *483*, 573–577.
11. Fu, X. Y.; Wang, Y.; Wu, N. Z.; Gui, L. L.; Tang, Y. Q. Surface Modification of Small Platinum Nanoclusters with Alkylamine and Alkylthiol: An XPS Study on the Influence of Organic Ligands on the Pt 4f Binding Energies of Small Platinum Nanoclusters. *J. Colloid Interface Sci.* **2001**, *243*, 326–330.
12. Jadzinsky, P. D.; Calero, G.; Ackerson, C. J.; Bushnell, D. A.; Kornberg, R. D. Structure of a Thiol Monolayer-Protected Gold Nanoparticle at 1.1 A Resolution. *Science* **2007**, *318*, 430–433.
13. Jiang, D. E.; Tiago, M. L.; Luo, W. D.; Dai, S. The "Staple" Motif: A Key to Stability of Thiolate-Protected Gold Nanoclusters. *J. Am. Chem. Soc.* **2008**, *130*, 2777–2779.
14. Guliamov, O.; Frenkel, A. I.; Menard, L. D.; Nuzzo, R. G.; Kronik, L. Tangential Ligand-Induced Strain in Icosahedral Au-13. *J. Am. Chem. Soc.* **2007**, *129*, 10978–10979.
15. Rodriguez, A.; Amiens, C.; Chaudret, B.; Casanove, M. J.; Lecante, P.; Bradley, J. S. Synthesis and Isolation of Cuboctahedral and Icosahedral Platinum Nanoparticles. Ligand-Dependent Structures. *Chem. Mater.* **1996**, *8*, 1978–1986.
16. Shafai, G.; Hong, S. Y.; Bertino, M.; Rahman, T. S. Effect of Ligands on the Geometric and Electronic Structure of Au-13 Clusters. *J. Phys. Chem. C* **2009**, *113*, 12072–12078.
17. Castro, E. G.; Salvatierra, R. V.; Schreiner, W. H.; Oliveira, M. M.; Zarbin, A. J. G. Dodecanethiol-Stabilized Platinum Nanoparticles Obtained by a Two-Phase Method: Synthesis, Characterization, Mechanism of Formation, and Electrocatalytic Properties. *Chem. Mater.* **2010**, *22*, 360–370.
18. Dablemont, C.; Lang, P.; Mangeney, C.; Piquemal, J. Y.; Petkov, V.; Herbst, F.; Viau, G. FTIR and XPS Study of Pt Nanoparticle Functionalization and Interaction with Alumina. *Langmuir* **2008**, *24*, 5832–5841.
19. Sen, F.; Gokagac, G. Activity of Carbon-Supported Platinum Nanoparticles Toward Methanol Oxidation Reaction: Role of Metal Precursor and a New Surfactant, tert-Octanethiol. *J. Phys. Chem. C* **2007**, *111*, 1467–1473.
20. Spivey, K.; Williams, J. I.; Wang, L. C. Structures of Undecagold Clusters: Ligand Effect. *Chem. Phys. Lett.* **2006**, *432*, 163–166.

21. Li, Y.; Galli, G.; Gygi, F. Electronic Structure of Thiolate-Covered Gold Nanoparticles: Au-102(MBA)(44). *ACS Nano* **2008**, *2*, 1896–1902.
22. Pei, Y.; Shao, N.; Gao, Y.; Zeng, X. C. Investigation Active Site of Gold Nanoparticle $Au_{55}(PPh_3)_{12}Cl_6$ in Selective Oxidation. *ACS Nano* **2010**, *4*, 2009–2020.
23. Mackay, A. L. A Dense non-Crystallographic Packing of Equal Spheres. *Acta Crystallogr.* **1962**, *15*, 916.
24. Pyykko, P. Relativistic Effects in Structural Chemistry. *Chem. Rev.* **1988**, *88*, 563–594.
25. Hakkinen, H.; Moseler, M.; Kostko, O.; Morgner, N.; Hoffmann, M. A.; von Issendorff, B. Symmetry and Electronic Structure of Noble-Metal Nanoparticles and the Role of Relativity. *Phys. Rev. Lett.* **2004**, *93*, 093401.
26. Huang, W.; Ji, M.; Dong, C. D.; Gu, X.; Wang, L. M.; Gong, X. G.; Wang, L. S. Relativistic Effects and the Unique Low-Symmetry Structures of Gold Nanoclusters. *ACS Nano* **2008**, *2*, 897–904.
27. Periyasamy, G.; Remacle, F. Ligand and Solvation Effects on the Electronic Properties of Au_{55} Clusters: A Density Functional Theory Study. *Nano Lett.* **2009**, *9*, 3007–3011.
28. Payne, M. C.; Teter, M. P.; Allan, D. C.; Arias, T. A.; Joannopoulos, J. D. Iterative Minimization Techniques for Abinitio Total-Energy Calculations - Molecular-Dynamics and Conjugate Gradients. *Rev. Mod. Phys.* **1992**, *64*, 1045–1097.
29. Blochl, P. E.; Forst, C. J.; Schimpl, J. Projector Augmented Wave Method: Ab initio Molecular Dynamics with Full Wave Functions. *Bull. Mater. Sci.* **2003**, *26*, 33–41.
30. Kresse, G.; Furthmuller, J. Efficient Iterative Schemes for Ab initio Total-Energy Calculations Using a Plane-Wave Basis Set. *Phys. Rev. B* **1996**, *54*, 11169–11186.
31. Perdew, J. P.; Wang, Y. Accurate and Simple Analytic Representation of the Electron-Gas Correlation-Energy. *Phys. Rev. B* **1992**, *45*, 13244–13249.
32. Apra, E.; Baletto, F.; Ferrando, R.; Fortunelli, A. Amorphization Mechanism of Icosahedral Metal Nanoclusters. *Phys. Rev. Lett.* **2004**, *93*, 065502-1–4.
33. Silvia, J. L.F.; Kim, H. G.; Piotrowski, M. J.; Prieto, M. J.; Tremiliosi-Filho, G. Reconstruction of Core and Surface Nanoparticles: The Example of Pt_{55} and Au_{55}. *Phys. Rev. B* **2010**, *82*, 205424.
34. Gronbeck, H.; Hakkinen, H.; Whetten, R. L. Gold-Thiolate Complexes Form a Unique c(4 × 2) Structure on Au(111). *J. Phys. Chem. C* **2008**, *112*, 15940–15942.
35. Grönbeck, H.; Walter, M.; Häkkinen, H. Theoretical Characterization of Cyclic Thiolated Gold Clusters. *J. Am. Chem. Soc.* **2006**, *128*, 10268–10275.
36. Templeton, A. C.; Wuelfing, W. P.; Murray, R. W. Monolayer-Protected Cluster Molecules. *Acc. Chem. Res.* **2000**, *33*, 27–36.
37. Hostetler, M. J.; Wingate, J. E.; Zhong, C. J.; Harris, J. E.; Vachet, R. W.; Clark, M. R.; Londono, J. D.; Green, S. J.; Stokes, J. J.; Wignall, G. D.; *et al*. Alkanethiolate Gold Cluster Molecules with Core Diameters from 1.5 to 5.2 nm: Core and Monolayer Properties as a Function of Core Size. *Langmuir* **1998**, *14*, 17–30.
38. Schmid, G. *Nanoparticles: From Theory to Application*; Wiley-VCH Verlag GmbH & Co. KGaA: Weinheim, 2006.
39. Li, Y.; Galli, G.; Gygi, F. Electronic Structure of Thiolate-Covered Gold Nanoparticles: Au(MBA). *ACS Nano* **2008**, *2*, 1896–1902.
40. Pei, Y.; Gao, Y.; Zeng, X. C. Structural Prediction of Thiolate-Protected Au: A Face-Fused Bi-icosahedral Au Core. *J. Am. Chem. Soc.* **2008**, *130*, 7830–7832.